Parsing of compositions and microstructure characteristics for rust-spots of pear pericarp

Lijun Nan [1,2,*], Shaobo Chen [1], Yashan Li [2], Ya Liu [1], Ying Jiang[1], Yan Yang [1], Chengdong Xu [2] and Guogang Chen [1,*]

[1] College of Food, Shihezi University, Shihezi, 832003 China

[2] School of Chemistry and Life Sciences, Chuxiong Normal University, Chuxiong, 675000 China

Abstract

The commercial value of Kurles pears pericarp, a popular and favored fruit for its unique aroma and refreshingly crisp texture, had sharply decreased because of a rust breakout of the beloved pear in China during the atmosphere-controlled storage. High performance liquid chromatography (HPLC) and liquid chromatography-mass spectrometry (LC-MS) were used to analyze rust spots on the pericarp of Kurle pears. Therefore, the chemical compounds of four various eluates, originating from the rust-colored substance

Received date:

Fund program: This work was supported by not only National Nature Science Foundation of China (30860181 and 31560468), but also 12th Five-Year Degree Authorized Construction Discipline in Biology of Yunnan Province, the Superior and Characteristic Discipline in Biology of Chuxiong Normal University (05YJJSXK03), University-level Academic Backbone Training Project for Chuxiong Normal College (XJGG1603), key major construction projects on “biotechnology” for Chuxiong Normal College.

Author: NAN Lijun (1973-), Man, Doctor, Research direction was focused on the grape physiology and wine production, E-mail: submit_paper73@126.com.

Corresponding author: CHEN Guogang, (1977-), Man, Doctor, Research direction was focused on the grape physiology and wine production, E-mail: submit_paper73@126.com.

NAN Lijun and CHEN Shaobo contributed equally to this paper for co-first author.

collected from the pears pericarp effected, were identified successfully for the first time, which were just rhein, aloe-emodin, chrysophanol and emodin, respectively. Taken together with microstructure characteristics for rust-spots of Kurle pear pericarp, it was no doubt that these eluates were the main factors affecting the rust spots on the pericarp of the Kurle pears during the atmosphere-controlled storage, which was a sign and consequence resisting the undesirable stress of the external environment.

Keywords: Chemical compounds, compositions analysis, microstructure, rust-colored substance, liquid chromatography-mass spectrometry, Kurle pear pericarp

Introduction

Besides of the grapes and apples, the pears are also the most popular temperate fruit species in China at present. Whereas there was an irrefragable fact that the pear industry had become financially burdensome recently due to be increasingly ruined by a number of the fungi diseases. In Europe, there was many reports about the pears having been perplexed by some sickness, such as the scab, powdery mildew, brown spots, fire blight, and other fungal diseases. Nevertheless, the pears had been suffering predominantly from the scab and rust caused by the black spot disease in Asia (Itai *et al.*, 2012), which had become the most significant trouble in term of the future of pear industry needing confront with the bravery.

As a rare species in the world, the Kurle pears were desired for the pure fragrance, refreshing juice, and tender quality and so on. The Kurle pears were frequently exported and highly sought after all throughout Southeast Asia and Europe nowadays. However, the frequent appearance of the rust spots on the pear cuticles had recently depreciated the commercial value of the fruits in a substantial way. Few studies had examined in detail this recent phenomenon affecting the exterior quality of this prized fruit (Liu *et al*., 2013; Stanislaw *et al*., 2015).

There were many methods available for the material analysis and identification until now, such as the chemical reaction, liquid chromatography (LC), gas chromatography (GC), thin layer chromatography (TLC), visible spectroscopy (UVC), liquid chromatography mass spectrometry (LC-MS), and nuclear magnetic resonance spectroscopy (NMRS). It was essential for us to choose an appropriate method analyzing and identifying the properties of the matter tested. To obtain the most accurate information about the experimental material, two or more methods of the analysis and identification should usually be adopted simultaneously. Thus, LC-MS and LC, as the combined methods, were chosen meanwhile in this trial to analyze and identify the rust spots of the Kurle pear, which would provide the theoretical basis as for the relevant technology controlling the rust spots on the Kurle pear pericarp.

In term of every creature, the cell was the basic unit of the organ and tissue performing the physiological function. Under the atrocious environmental stimulation

inevitably, the combined action between the broken cell wall and the lignification reaction inside the cell formed the cork cambium from the pear peel of the rusty spot (Clairmont *et al*., 1992). The thin epidermal cells of the fruit peel were damaged easily and developed quickly the cork layer under the stimulation of the severe environment, while the cork cell accumulating on the skin developed the terrible rusty spot. As we all known, there were a lot of the rough endoplasmic reticulum in the plant epidermal cell, which was the source of many organelles, such as the vacuoles and golgi apparatus, whereas the material transportation between the cells could been regulated constantly and steadily by the biochemical process of the endoplasmic reticulum. Two experiments of Teasdale and Jackson (1996) and Xie *et al*. (2009) had demonstrated that the endoplasmic reticulum was not obvious degradation role during the fruit maturation excluding the final stages of the overripe. In view of these conclusions, the analysis of the ultramicroscopic structure, as far as the rusty spot area and intact cells of the korla fragrant, could lay a foundation for the identification of the rusty spot material.

Materials and methods

Sampling and treatment of fruits

The Kurle pears used in this study, kept in atmosphere-controlled storage, were sampled according to the concrete experiment demands on Novermber 22, 2015 from Kurle city, China, respectively.

The fresh - keeping storehouse with the atmosphere - controlled function, 50 m^2, stored 10,000 Kg of the Kurle pears, which were kept in 4 m hight, 50 cm altitude per storey of goods shelf, and a layer of pear in every storey of good shelf, of storage rack. 10 Kg parent population of fruits per replication were sampled randomly from the middle and four sides of the storeroom. Classification, 4 sorts, was carried out according to the shape and color of the rust spot, excluding a sigle of the same category without the defect of the fruit. 10 fruits, the similar shape and color of the rust spot, were pooled to obtain one sample for the analysis. All factors was repeated three times.

The 5 g samples of the rust spots per sort above, treated with a 125 mL ethanol (70%) solution after weighed accurately, were extracted from the surface of the pears. Then, the liquid extracted was concentrated immediately to a ratio of 1: 4 after being eluted with the petroleum ether - acetone and petroleum ether - ethyl acetate gradient elution further, which were named elution 1, elution 2, elution 3 and elution 4, respectively. Additionally, the reagents of the chloroform and petroleum ether were added as another extraction liquid (EL) of the extraction agents with water (EL : water =1: 1).

Finally, the rust spots liquids of the pears above were separated and purified with the method of the column chromatography, respectively. The procedure was listed as follows. Firstly, the petroleum ether extract was washed by the mixtures of the petroleum ether and acetone with two different ratios of the eluates (4: 1, 5: 1),

97 respectively. The elution 1 was collected in the cyclone separator of the extraction
98 unit. Secondly, the chloroform extract was washed with the mixtures of the petroleum
99 ether and ethyl acetate with three different gradients of the eluates (5: 1, 4: 1 and 2: 1),
100 respectively. In addition, the samples, namely elution 2, 3 and 4, were also collected
101 in the cyclone separator of the extraction units, respectively. It was vigilant that the
102 liquid level, not less than the upper surface of the quartz sand, was always ensured
103 during the chromatographic separation experiment, and the cock of the
104 chromatography column should be closed in time before the samples were added. In
105 addition, it should be noticed that the dropper should not bring into contact with the
106 upper surface of the quartz sand until the samples were injected continually, while the
107 cock of the chromatography column must be immediately opened after finishing the
108 sample injection. At alst, the eluting agent was collected smoothly and continuously
109 within a 2 - mL bottle numbered at the rate of 5 - 8 drops per minute, respectively,
110 and prepared for the test of the purity.

111 *Samples analysis of LC - MS*

112 The samples, including elution 1, elution 2, elution 3 and elution 4, were
113 analyzed with LC - MS, respectively. The analysis conditions were as follows: mobile
114 phase (firstly 0.1% of 100% formic acid, 10 min; followly 0.1% miscible liquids of
115 40% acetonitrile + 60% formic acid, 20 min; finally 100% acetonitrile, 8 min),
116 column temperature (45 ℃), wavelength (200 - 400 nm), flow velocity (0.3 mL/min),
117 sample volume (1 μL); ion form (ESI^- and ESI^+), capillary voltage (3.0 and 3.5

118 kVolts), cone voltage (20 and 20 Volts), ion source temperature (100 ℃ and 100 ℃
119), desolvation temperature (250 ℃ and 250 ℃), removal of solvent gas flow (500
120 and 500 lit/hr), conical flow (50 and 50 lit/hr), collision energy (15 and 15 Volts),
121 mass range (100 - 1500 and 100 - 1500 m/z), detector voltage (1700 and 1600 Volts).

122 *Samples analysis of LC*

123 The another samples, elution 1, elution 2, elution 3 and elution 4, were analyzed
124 with LC referring to the standard mixture of both Li *et al*. (2011) and Purnhauser *et al*.
125 (2011). The experimental conditions were as follows: mobile phase (Methanol: 0.1%
126 Phosphoric acid) = 85: 15, column temperature 25 ℃, wavelength 254 nm, flow
127 velocity 0.3 mL/min, sample volume 20 μL. A qualitative analysis was also
128 performed in accordance with the standard mixture and retention time of the four
129 elution solutions.

130 *Ultrastructure of fragrant pear cell*

131 The intact parts of the Kurle pears was taken as control to illuminate and
132 ascertain the microstructure characteristics of the rusty spot of the experimental
133 material during the atmosphere - controlled storage. 3% glutaraldehyde solution was
134 configured by 0.05 mol/L phosphate buffer (pH 6.8) first. The peel and pulp of the
135 fragrant pear, cut into 1 mm x 2 mm (longth x width) wafer by the scalpel, was fixed
136 24 h with 3% glutaraldehyde solution under 4 □ before being rinsed 3 - 4 times with
137 phosphate buffer (pH 6.8). After that, the samples, fixed 2 h by 1% osmic acid
138 solution at room temperature, followed 30%, 50%, 60%, 70%, 80%, 90% and 100%

ethanol dehydration in gradient, 15 minutes each time after being also washed 3 - 4 times by the phosphate buffer (pH 6.8), respectively. The materials above were successfully replaced three times with the acetone further, then embedded both about 2 h by the embedding medium (acetone: epoxy resin = 3: 1) and over 4 h with the medium (acetone: epoxy resin= 1: 1), respectively, prior to the polymerization of the temperature - keeping box at 60 □ for 24 h. Finally, the polymerized samples were sliced into the slices (about 60 nm of thickness) with the ultra - thin slicing machine in order to the observation and photograph under the transmission electron microscope.

Instruments and equipments

Instruments and equipments in the trial was readied as follow:

Hitachi H - 600 transmission electron microscope, OLYMPUS CX21FS1 optical microscope, 705902 ultra - thin slicing machine (leica in Australia), HPLC (LC - 2010A, Shimadzu, Japan), LC - MS (LCMS8030, Shimadzu, Japan), chromatograph (Waters acquity uplc), detector (Waters acquity pda), and analytical column (BEH, C18, 2.1×100 mm 1.7 μm).

Reagents

Instruments and equipments in the trial included: methanol (GR, Fair Lawn, USA), acetonitrile, rhein, chrysophanol, aloe emodin and emodin (GR, Sigma, USA). phloroglucinol, safranine, 95% ethanol, osmic acid, iodine, potassium iodide, glutaraldehyde, epoxy resin and phosphoric acid (AR, BASF, Tianjin), formic acid (AR, Xi'an Chemical Reagent Factory).

Results

LC-MS analysis of Elution 1

According to the mass spectrum (Fig. 1), the molecular weight of the elution 1 was 284. The mass spectral information, m/z, was as follows: 283 [M^+], 239 [M^+ - COOH], 211 [M^+ - COOH - CO], 183 [M^+ - COOH – CO - CO]. In comparison with the prototype HPLC information under the same chromatographic conditions, the identification result showed that the retention times were fairly consistent in regard to the elution 1 (25.055 min) and rhein standard (25.068 min) (Fig. 5a and 5b). Based on the analysis above, it was quite obvious that the elution 1 could be identified as rhein, and molecular structure of which was displayed in Fig. 6a.

LC-MS analysis of Elution 2

The molecular weight of the elution 2, 270, could be also seen in Fig. 2, and the results of the mass spectral information (m/z) included: 270 [M^+], 269 [M^+ - H], 241 [M^+ - CO - H], 223 [M^+ - 2H - COOH], 195 [M^+ - 2H – COOH - CO], 183 [M^+ - COOH – CO - CH_2]. Through the prototype HPLC information under the same chromatographic conditions, the retention times of the identification result were fairly the same as the elution 2 (18.998 min) and aloe emodin standard (18.981 min) (Fig. 5a and 5c). Based on the fact above, the elution 2 was ascertained as aloe emodin, and molecular structure of which was showed in Fig. 6b.

LC-MS analysis of Elution 3

According to Fig. 3, the molecular weight of the elution 3 was 254. The mass spectral information was as follows (m/z): 254 [M^+], 253 [M^+ - H], 225 [M^+ - COH], 162 [M^+ - 2COH - 2OH], 158 [M^+ - COH – CO -3CH]. The prototype HPLC information was referred to as the control under the same chromatographic conditions, the fairly consistent retention times, the elution 3 (44.028 min) and chrysophanol standard (43.948 min), were found in Fig. 5a and 5d. Therefore, the elution 3 was affirmed unquestionably as the chrysophanol, and the molecular structure of which was showed in Fig. 6c.

LC-MS analysis of Elution 4

It was satisfied that the molecular weight of the elution 4, 270, could be also obtained based on Fig. 4. The mass spectral information was distinct (m/z): 270 [M^+], 269 [M^+ - H], 241 [M^+ - CO - H], 225 [M^+ - CO - OH], 197 [M^+ - 2CO - OH]. Analyzing the prototype HPLC information, the retention times of both the sample (35.177 min) and the standard reagent (35.022 min) under the same chromatographic condition. Through the summary on the above analysis, the elution 4 was identified as the emodin (Fig. 5a and 5e), and the molecular structure of which was displayed in Fig. 6d.

Discussion

LC - MS analysis of Elution 1

From the more careful check, there was a the most pleasant surprise that the result was in accordance with the previous data about the mass spectrum of the rhein

(Doğmuş-Lehtijärvi *et al*., 2009; Brewer *et al.*, 2009; Douglas *et al*., 2010; Mathias *et al*., 2011).

Rhein was thought of as the anthraquinone compounds (Cben *et al*., 2011). Anthraquinone ring containing two hydroxyl and a carboxyl possessed the stronger polarity and the characteristics of a strong oxidation reduction. Therefore, the rhein was not stable very much, and decomposed easily by the oxidation - reduction reactions. Rhein, based on the fact above, should be fond of the anaerobic environment. The controlled atmosphere storage method, adopted in this experiment created exactly an anaerobic environment for the fragrant pear, could resist effectively the oxidation of the external environment. As we all known, the rhein could provide some roles, such as the antibacterial and scavenging free radicals (Rodríguez *et al*., 200). Therefore, the rhein was advantageous to the storage of the fragrant pear owe to protecting the organization from the damage. Some measures, such as increasing the light intensity, raising the temperature and improving pH, could accelerate the degradation rate of the rhein with the degradation reaction of the first order kinetics process. When the pH > 8, the reaction rate of the rhein degradation would increase rapidly. So the rhein was more suitable for a cool environment avoiding the violent glare and stronger alkaline environment. This fragrant pear with a certain acidity, adopting the controlled atmosphere storage, was conserved in the lower temperature, oxygen free or micro oxygen environment in the trial, therefore, the rhein could be

221 easily detected inevitably, which was also the embodiment of the korla fragrant pear
222 with a strong antioxygenic property.

223 *LC - MS analysis of Elution 2*

224 Beyond all reasonable doubt that the results of the mass spectral information in Fig. 2
225 was consistent with the previous datas for aloe emodin (Crampton *et al*., 2009;
226 Doğmuş-Lehtijärvi *et al*., 2009; Brewer *et al*., 2009; Douglas *et al*., 2010; Mathias *et*
227 *al*., 2011; Itai *et al*., 2012).

228 Aloe emodin belonged to anthraquinone compound, which usually existed in
229 Chinese herbal medicine, such as aloe, rhubarb and cassia seed. This experiment also
230 detected the aloe emodin in the korla fragrant pear. The effective antibacterial
231 ingredients of the aloe emodin possessed some obvious features, such as the anti -
232 tumor activity, antibacterial activity and immunosuppression and purgation (Li *et al*.,
233 2012; Hu *et al*., 2014). Therefore, the aloe emodin in the korla fragrant pear had
234 played a part in the certain antibacterial activity to the pear fruit, the body function
235 could be improved obviously after the korla fragrant pear with the aloe emodin was
236 eated. The pharmacological activity of the aloe emodin was related closely to the
237 chemical structure of the aloe emodin itself. An anthraquinone ring and two phenolic
238 hydroxyl of which determined the function of the biological activities including the
239 removal of the oxygen free radicals, antitumor and other aspects (Ruie *et al*., 2014).
240 Another study demonstrated yet that the aloe emodin could enhance the phagocytosis
241 of the macrophage, and induce the mRNA expression of the cytokines including

242 interleukin in the white blood cells, except for the tumor necrosis factor and interferon
243 (Yu *et al*., 2006) so as to enhance the body's immune function. Therefore, the aloe
244 emodin contained could protect the skin of the korla fragrant pear from the erosion of
245 the foreign organisms. Under the condition of the controlled atmosphere storage in
246 this trial, the skin of the korla fragrant pear would generate spontaneously the aloe
247 emodin, which was a reflection of the adaptability characteristic to resist the external
248 environment for the korla fragrant pear.

249 *LC - MS analysis of Elution 3*

250 A delirious and unavoidable fact was that the mass spectral information in Fig. 3 and
251 the prototype HPLC information in Fig. 5a and 5d in the trial were in accord with the
252 previous data for chrysophanol (Manjunatha *et al*., 2008).

253 It was all known that the chrysophanol belonged also to the anthraquinone
254 compounds. The chrysophanol could fight availably against the apoptosis by means of
255 improving the mitochondrial activity and the steady - state of the cell membrane,
256 which was beneficial to the antiapoptotic impact of the hypoxia injury cells. After the
257 hypoxia injury, there was a prominent variation for the permeability of the cell
258 membrane on the cell surface. The augmentation of the cell damage degree promoted
259 the reinforce of the permeability on the cell membrane, as well as the increase of the
260 release quantity and synthetic level. A large number of the experimental results
261 showed that the rhubarb phenol could improve the permeability of the cell membrane
262 through the stability of the cell membrane, and stabilize the internal environment in

the cell further, which reduced the damage level of the hypoxic cells significantly, enhanced the resistance ability on the hypoxia as for the cell self. In this experiment, the existence of the rhubarb phenol in the fragrant pear skin could improve significantly the permeability of the skin cell membrane, meanwhile stable the inner environment in the cell. Thus, the anoxic environment created by the controlled atmosphere storage could make the damage extent of the hypoxic cells on the fragrant pear skin reduce quickly to a minimum degree, which was favorable to enhance the cell's ability to resist the hypoxia condition. Therefore, the rhubarb phenol had an advantage obviously role for the freshness of the korla fragrant pear, which could prolong the shelf life of the korla fragrant pear.

LC - MS analysis of Elution 4

The fact, on the LC - MS analysis on Fig. 4 and the prototype HPLC information of Elution 4 in Fig. 5a and 5e, was agreed with the previous records for emodin (Ranjini *et al*., 2011; Chen *et al*., 2012)

As three elutions above, the emodin detected from the elution 4 was also a kind of the anthraquinone active substance with the typical structure of 9, 10 - anthraquinone. Therefore, the emodin displayed just more stablility at the highest oxidation levels. Previous studies had shown that the emodin had an important role in some aspects, such as the anti - cancer, anti - inflammatory, antibacterial, antiviral, anti - oxidation and purgative activity (Yan *et al*., 2014). Antibacterial mechanism of the emodin had to do with the electron transfer inhibiting the mitochondrial

284 respiratory chain and breath, including the oxidation and dehydrogenation of the
285 metabolism intermediates from the amino acid, sugar, and protein. Emodin could
286 inhibit the growth of the bacteria by adjusting the ultima synthesis of the nucleic acid
287 and protein. In this experiment, the emodin on the korla fragrant pear skin could
288 inhibit the electron transfer of the mitochondrial respiratory chain and the breath of
289 the epidermal cells, including the oxidation and dehydrogenation of the metabolism
290 intermediates from the amino acid, sugar, and protein of the pidermal cells, restrain
291 the microbial activity of the korla fragrant pear skin eventually in order to achieve the
292 goal of the preservation quality on fragrant pear.

293 In addition, emodin, as a natural inhibitors, had also certain inhibitory effect on
294 the non - enzymatic glycosylation system. In the initial stage, the emodin could inhibit
295 the condensation and cyclization of the carbonyl of the glucose and the amino of
296 lysine from the fructosamine. The fructosamine after the amadori rearrangement was
297 cracked into the dicarbonyl compounds promoting the obvious inhibitory effect on the
298 glyoxal again after the enolization, which was a sign entering the middle stage of the
299 non - enzymatic glycosylation system. Finally, the dicarbonyl compound and amino
300 compound were polymerized into the final product by the polymerization of the
301 aldehyde group and amino group. While the emodin had better inhibition role for
302 these products including the carboxymethyl lysine (CML) and the melanoidin. In the
303 process of the reaction, glyoxal, as a precursor of the carboxymethyl lysine, could be
304 generated easily by the autoxidation of the glucose, or by the oxidation of the

305 intermediate coming from the maillard reaction. So the emodin could suppress
306 significantly the glycosylation through the antioxidation function. In addition, the
307 emodin had no obvious inhibition influence to the intermediate, 5 - hydroxymethyl
308 furfural, of the maillard reaction, which was confirmed further to the fact above. Thus,
309 the emodin detected in this experiment endowed a strong antioxidant capacity to the
310 skin of the korla fragrant pear, which could improve a capacity resisting the
311 alternation of the external environment. In consequence, the existence of the emodin
312 was conducive to the preservation of the fragrant pear.

313 In sum, the main bioactive constituents originating from the rust - colored
314 substance collected from the pericarp of the Kurle pear were anthraquinones, namely
315 aloe - emodin, rhein, emodin and chrysophanol (Fig. 5f), respectively, based on the LC
316 - MS analysis combining with the studied results previously.

317 *Function of related anthraquinone*

318 These anthraquinones synthesized via the polyketide pathway, such as emodin,
319 chrysophanol, rhein, aloe - emodin, and physicione, were of the hydrophobic and a
320 large number of the biological function, such as the anticancer (Shoemaker *et al*., 2005;
321 Huang *et al*., 2007), antimicrobial and anti - inflammatory (Fosse *et al*., 2004; Tseng
322 *et al.*, 2006).

323 Research had demonstrated that the emodin was an effective inhibitor of the *neu*
324 and *ras* oncogenes in vitro of kinase enzyme (Chang *et al*., 1996), while emodin,
325 together with anthraflavic acid, had also exhibited amicable protection mechanism

326 against the benzo(a)pyrene mutagenicity and dietary pyrolysis mutagens through the
327 Ames bacterial mutagenicity assay (Ayrton *et al*., 1988; Lee *et al*., 1991). It was
328 interested that the orange aloe - emodin could induce the micronucleus frequencies in
329 the mouse lymphoma L5178Y cells in the *in vitro* micronucleus test (Frisvad 1989),
330 and the fungal chrysophanol were also considered as the mycotoxins owe to the violent
331 genotoxicity today (Mueller *et al.*, 1998). Thus the detection of the emodin,
332 chrysophanol, rhein, aloe - emodin and physicione suggested that some of these fungi
333 possessed usually potent mycotoxigenic. Research result, however, about $CaCl_2$ and
334 pullulan treatments improving and even inhibiting the development degree of the
335 brown spots on 'Huangguan' pear by delaying the loss of the polyphenol substances
336 and maintaining the structural integrity of the cell membrane (Kou *et al*., 2015)
337 provided really a train of thoughts for the further research about the relationships
338 between the pullulan and the aloe - emodin, rhein, emodin and chrysophanol. In this
339 study, HPLC and LC - MS were used to analyze the rust spots on the pericarp of
340 Kurle pears. As a result, four elutions (elutions 1 to 4), the material sources of the rust
341 spots, were identified as rhein, aloe - emodin, chrysophanol and emodin, respectively,
342 which was similiar to previous works(Kou *et al*., 2015), and also provided a
343 foundation for the future study of the rust spots.

344 *Ultrastructure of rusty spot and intact parts*

345 The rusty spot parts of the korla fragrant pears had irregular black shadows, while the
346 intact ones of which was white and transparent under the transmission electron

347 microscopy (TEM) (Fig. 6). From Figs. 6d and 6e, the cell membrane and cell wall of
348 the rusty spot sections was disappearing gradually with the serious damage of the cell
349 wall, which led to the unclear cell contour ultimately. Therefore, there was not nearly
350 a complete cell in the pears surface with the rusty spot. Another, the irregular black
351 substance could be simultaneously and clearly found in the cell. Moreover, the
352 ultrastructure of the avocado fruit cell had been observed during the mature process
353 with the electron microscope. During the sclereid period, the intercellular layer,
354 including each side ranged the filaments closely, of the fruit cells was clearly visible.
355 However, the fruits accelerating the decrepitude promoted the gradual disintegration
356 of the filaments and intercellular layer in the cell after the respiration peak (Ruth *et al*.,
357 1979; Chatelet *et al*., 2008), which was similar to the some conclusions, such as the
358 damage of the cellular structure, the autolysis of the intercellular layer, as well as the
359 rusty spot being gradually formed on the korla fragrant pear after the respiratory
360 climacteric during the postharvest storage. However, the important information
361 supplied stemming from Fig. 6c and 6f showed that the cells were enough intact, oval
362 and rowed neatly, and the outline of the cell wall was also distinct enough.

363 The black shadow, differ from that of the rusty spot section but integrated cell
364 membrane and cell wall, of Fig. 6o was regular, which was induced by the
365 mitochondria. The chrysophanol could adjust the mitochondria function, while the
366 antibacterial mechanism of the emodin had to do with the electron transfer inhibiting
367 the mitochondrial respiratory chain and breath, including the oxidation and

368 dehydrogenation of the metabolism intermediates from the amino acid, sugar, and
369 protein. However, the mitochondria of hwangkumbae, the clear double structure in
370 internal envelope, and most of the round or oval shape, grew in the cell wall or next to
371 a plasmid during the young fruit period (Cuthbertson *et al*., 2003). From Fig. 6m,
372 there were still part of the cell inclusions in the rust stain section of the korla fragrant
373 pear, mitochondria, but without the organelles, such as the endoplasmic reticulum,
374 golgi apparatus and microbody because of the mitochondrial more resistance collapse,
375 could sometimes continue until the senescence phase, than the other micro.
376 Meanwhile, the change of the mitochondrial membrane, such as the swelling, formed
377 the cavity and destruction of the structure, led to gradually breaking apart of the
378 mitochondria. Mitochondria were an important energy converter of the fruit cell. As
379 we all known, the energy of the cells were supplied mainly by the mitochondria on the
380 storage duration after the harvest. So, with the apolexis of the fruit, the fewer the
381 number of the mitochondria was, the less the energy in cells would be, which abated
382 correspondingly the repair and synthetic capacity of the cell, accelerated the collapse
383 of the cell membrane, and even cell death finally (Chatelet *et al*., 2008).

384 As could be seen from Fig. 6, there were black substances deposited in the skin
385 cell during the formation of the rust stain. With the continued expansion of the pear
386 rust stain area, these black materials began to extend gradually from the gap between
387 the cells to the intracellular space, and even until the whole cell. At this time, the dark
388 brown spots or patches in the pear skin were continuously extended likewise. It was

389 interesting that during the late period of the pear storage, the number of the ribosome
390 in rusty spot cells began to reduce gradually with the degeneration of the chloroplast
391 badly destroyed, while the endoplasmic reticulum and golgi apparatus was rapidly
392 disintegrated or collapsed owe to the vesiculation. At last, the tendency that the
393 mitochondria began to collapse with the collapsed tonoplast before the microorgans
394 were disintegrated completely became irreversible really, which led inevitably to the
395 damage of the cytoplasm membrane further, and the death of the cells ultimately.
396 Once the structure of the cell was destructed, some requirements, such as the
397 dissociation of the intracellular phenols, as well as the increase of the phenylalanine
398 ammonia enzyme and polyphenol oxidase activity, generated the dark brown
399 substances under the interaction between these enzymes and phenolic substrates. With
400 the destruction of the cell structure, these substance were still persistently increasing
401 until the whole cell, which was the whole evolutionary process of the rusty spot
402 development. The study of Cuthbertson and Murchie (Cuthbertson *et al*., 2003) found
403 that during the formation of the rusty spot on the hwangkumbae, the cell suberized
404 stage by stage with the deepened color of the rusty spot gradually, but there was lack
405 cause definitely now. Whereas we could see from the trial, there was a reasonable
406 reason originating from the enzymatic browning. All in all, the combined action,
407 namely both the stimulation under the adverse environment accelerated the maturation
408 and aging of the pear, and the damage and collapse of the intracellular organelles to a

409 variable extent, induced or launched the complicated physiological and biochemical
410 process during the whole period.

411 The microstructure characteristic of Korla fragrant pear with the rusty spot and
412 without the intact parts showed advantageously that the cytomembrane and cytoderm
413 of the rusty spot location was bit by bit disappearing, while other organelles, such as
414 the mitochondria, endoplasmic reticulum and golgi apparatus, were gradually
415 disintegrated. As a result, the extended range and degree of the black deposits were
416 increased abidingly from the local of the cells to the whole ones, it was without doubt
417 which was an overt sign against the emergency response outside the environmental
418 damage as for the skin of the fragrant pear, supported also by some conclusions on the
419 eluent in the trial above (Fig. 1 - 5). But the fact we couldnot ignore was that the
420 intact position was not an object of the microbial invasion, or not easy to be invaded
421 by the microbes owe to the integral structures including some properties, such as the
422 organizational hardness, structural material, enzyme activity of the peel, as well as
423 some factors including the lower conditions of the environmental temperature created
424 by the controlled atmosphere storage and the qualified sanitary condition. Therefore,
425 there were no loss of the substances between and in cells, and the rust spots with the
426 defensive function were not come into being on the surface of the peel (Fig. 6c, f, i, l,
427 and o). Naturally, There were not four anthraquinones, including aloe - emodin, rhein,
428 emodin and chrysophanol on the surface of the unbroken peel. Thus, not only the
429 damage of the cell structure on the pear skin, but also the increase of the lignin and

430 secondary protection organization of the intercellular layer, including the further
431 lignification of the secondary organization led to the formation of the rusty spot
432 finally, which postponed the senescence of the pear fruit further.

433 **Conclusion**

434 In conclusion, the main rust - colored substance originating from the bioactive
435 constituents collected from the pericarp of Kurle pear were anthraquinones, including
436 aloe - emodin, rhein, emodin and chrysophanol. Another, the microstructure
437 information obtained from the rusty spot and intact parts in Korla fragrant pear drew a
438 prominent conclusion that the gradual variation of some organelles, such as the
439 cytomembrane, cytoderm, mitochondria, and endoplasmic reticulum of the rusty spot
440 location resulted in the abiding expansion of more and more black deposits toward the
441 whole cells. The damage of the cell structure on the pear skin, as well as the increase
442 of the lignin and secondary protection organization, including the further lignification
443 organization, in the intercellular layer, led to the formation of the rusty spot finally,
444 which was the result of the self - defence against the harsh environment.

445 **References and Notes**

446 **Ayrton AD, Ioannides C, Walker R**. 1988. Anthraflavic acid inhibits the
447 mutagenicity of the food mutagen IQ: mechanism of action. *Mutation Research Letters.*
448 **207(3)**, 121-125.

449 **Brewer LR, Alspach PA, Morgan C, Bus VGM**. 2009. Resistance to scab caused by
450 Venturis pirina in interspecific pear (Pyrus spp.) hybrids. *New Zealand Journal of*
451 *Crop and Horticultural Science* **37(3)**, 211-218.

452 **Cben WH，Cben J，Sbi YP**. 2011. Antbraquinones and stilbenes from tbe roots and
453 rbizomes of Rbubarb. *Journal of Asian Natural Products Research* **13(11)**,
454 1036-1041.

455 **Chang CJ, Ashendel CL, Geahlen RL, McLaughlin JL, Waters DJ.** 1996.
456 Oncogene signal transduction inhibitors from medicinal plants. *In Vivo (Athens,*
457 *Greece)* **10(2)**, 185-90

458 **Chatelet DS, Rost TL, Matthews MA, Shackel KA.** 2008. The peripheral xylem of
459 grapevine (Vitis vinifera) berries. 2. Anatomy and development. *Journal Of*
460 *Experimental Botany* **59(8),** 1997-2007.

461 **Chen RI, Zhang JM, Hu YY, Wang YT**. 2014. Potential Antineoplastic Effects of
462 Aloe-emodin: A Comprehensive Review. *The American Journal of Chinese Medicine*
463 *42(2)*, 275-288.

464 **Chen ZY, Brown R, Menkir A, Cleveland T**. 2012. Identification of
465 resistance-associated proteins in closely-related maize lines varying in aflatoxin
466 accumulation. *Molecular Breeding* **30(1)**, 53-68.

467 **Clairmont CA, De Maio A, Hirschberg CB.** 1992. Translocation of ATP into the
468 lumen of rough endoplasmic reticulum-derived vesicles and its binding to luminal

proteins including BiP (GRP 78) and GRP 94. *Journal of Biological Chemistry* **267**, 3983-3990.

Crampton BG, Hein I, Berger DK. 2009. Salicylic acid confers resistance to a biotrophic rust pathogen, Puccinia substriata, in pearl millet (Pennisetum glaucum). *Molecular Plant Pathology* **10,** 291-304.

Cuthbertson AGS, Murchie AK. 2003. The impact of fungicides to control apple scab (*Venturia inaequalis*) on the predatory mite Anystis baccarum and its prey Aculus schlechtendali (applerust mite) in Northern Ireland Bramley orchards. *Crop Protection* **22(9)**, 1125-1130.

Doğmuş-Lehtijärvi H, Lehtijärvi A, Aday A. 2009. European pear rust on Juniperus excelsa L. in south-western Turkey. *Forest Pathology* **39**, 35-42.

Douglas GL, Michael BM, Melissa LC, Laurie LF, Alberto N. 2010. Proteomic analysis of germinating urediniospores of Phakopsora pachyrhizi, causal agent of Asian soybean rust. *Proteomics* **10(19),** 3549-3557.

Fosse C, Le Texier L, Roy S, Delaforge M, Grégoire S, Neuwels M, Azerad R. 2004. Parameters and mechanistic studies on the oxidative ring cleavage of synthetic heterocyclic naphthoquinones by Streptomyces strains. *Applied Microbiology And Biotechnology* **65(4)**, 446-456.

Frisvad JC. 1989. The connection between the Penicillia and Aspergilli and mycotoxins with special emphasis on misidentified isolates. *Archives of Environmental Contamination & Toxicology* **18(3)**, 452-467.

Hu B, Zhang H, Meng X, Wang F, Wang P. 2014. Aloe-emodin from rhubarb (rheum rhabarbarum) inhibits lipopolysaccharide-induced inflammatory responses in raw264.7 macrophages. *Journal of Ethnopharmacology* **153(3)**, 846-53.

Huang Q, Lu G, Shen HM, Chung MC, Ong CN. 2007. Anti-cancer properties of anthraquinones from rhubarb. *Medicinal Research Reviews* **27(5),** 609-630.

Itai A, Igori T, Fujita N, Egusa M, Kodama M, Murayama H. 2012. Ethylene analog and 1-Methylcyclopropene enhance black spot disease development in Pyrus pyrifolia Nakai. *HortScience* **47(2)**, 228-231.

Kou XH, Wu MS, Li L, Wang S, Xue ZH, Liu B, Fei YQ. 2015. Effects of $CaCl_2$ dipping and pullulan coating on the development of brown spot on 'Huangguan' pears during cold storage. *Postharvest Biology & Technology* **99,** 63-72.

Lee H, Tsai SJ. 1991. Effect of emodin on cooked-food mutagen activation. *Food and Chemical Toxicology* **29(11),** 765-770.

Li HB, Wei GR, Xu JR, Huang LL, Kang ZS. 2011. Identification of wheat proteins with altered expression levels in leaves infected by the stripe rust pathogen. *Acta Physiologiae Plantarum* **33(6)**, 2423-2435.

Li Y, Xu Y, Lei B, Wang W, Ge X, Li J. 2012. Rhein induces apoptosis of human gastric cancer sgc-7901 cells via an intrinsic mitochondrial pathway. *Brazilian Journal of Medical & Biological Research* **45(11),** 1052-1059.

Liu P, Xue C, Wu TT, Heng W, Jia B, Ye Z, Liu L, Zhu L. 2013. Molecular analysis of the processes of surface brown spot (SBS) formation in pear fruit (Pyrus

bretschneideri Rehd. cv. Dangshansuli) by de novo transcriptome assembly. *PloS one* **8(9)**, e74217.

Manjunatha G, Raj SN, Shetty NP, Shetty HS. 2008. Nitric oxide donor seed priming enhances defense responses and induces resistance against pearl millet downy mildew disease. *Pesticide Biochemistry & Physiology* **91(1),** 1-11.

Mathias DeB, Hossein A, Erik VB, Isabel RR,Theo VDL, Martine M, Kurt H. 2011. Identification and characterization of pathotypes inPuccinia horiana, a rust pathogen of Chrysanthemum xmorifolium. *European Journal of Plant Pathology*. **130(3)**, 325-338.

Mueller SO, Stopper H, Dekant W. 1998. Biotransformation of the anthraquinones emodin and chrysophanol by cytochrome P450 enzymes bioactivation to genotoxic metabolites. *Drug Metabolism and Disposition* **26(6)**, 540-546.

Purnhauser L, Bóna L, Láng L. 2011. Identification of Sr31 and Sr36 stem rust resistance genes in wheat cultivars registered in Hungary. *Cereal Research Communications* **39**, 53-66.

Ranjini P, Shailasree S, Kini KR, Shetty HS. 2011. Isolation and characterisation of a NBS-LRR resistance gene analogue from pearl millet. *Archives of Phytopathology & Plant Protection* **44 (10)**, 1013-1023.

Rodríguez J, Olea-Azar C, Cavieres C, Norambuena E, Delgado-Castro T, Soto-Delgado J, Araya-Maturana R. 2007. Antioxidant properties and free

radical-scavenging reactivity of a family of hydroxynaphthalenones and dihydroxyanthracenones. *Bioorganic & Medicinal Chemistry* **15(22)**, 7058-7065.

Ruth BA, Naomi K, Chaim F. 1979. Ultrastructural changes in the cell walls of ripening apple and pear fruit. *Plant Physiology* **64(2),** 197-202.

Shoemaker M, Hamilton B, Dairkee SH, Cohen I, Campbell MJ. 2005. In vitro anticancer activity of twelve Chinese medicinal herbs. *Phytotherapy Research* **19(7),** 649-651.

Stanislaw K, Jan O, Aneta W. 2015. Increased content of phenolic compounds in pear leaves after infection by the pear rust pathogen. *Physiological and Molecular Plant Pathology* **91**, 113-119.

Teasdale RD, Jackson MR. 1996. Signal-mediated sorting of membrane proteins between the endoplasmic reticulum and the goldi apparatus. *Annual Review of Cell and Developmental Biology* **12(11),** 27-54

Tseng SH, Lee HH, Chen LG, Wu CH, Wang CC. 2006. Effects of three purgative decoctions on inflammatory mediators. *Journal Of Ethnopharmacology* **105(1-2)**, 118-124.

Xie ZS, Charles FF, Xu WP, Wang SP. 2009. Effects of Root Restriction on Ultrastructure of Phloem Tissues in Grape Berry. *HortScience*. **44(5),** 1334-1339.

Yan TC, Bo L, Jun X, Pao X, Habte-Tsion HM, Zhang YY. 2014. The effect of emodin on cytotoxicity, apoptosis and antioxidant capacity in the hepatic cells of grass carp (*Ctenopharyngodon idellus*). *Fish & Shellfish Immunology* **38(1)**, 74-79.

552 **Yu CS, Yu FS, Chan JK, Li TM, Lin SS, Chen SC, Hsia TC, Chang YH, Chung**

553 **JG.** 2006. Aloe-emodin affects the levels of cytokines and functions of leukocytes

554 from Sprague-Dawley rats. *In Vivo.* **20(4),** 505-509.

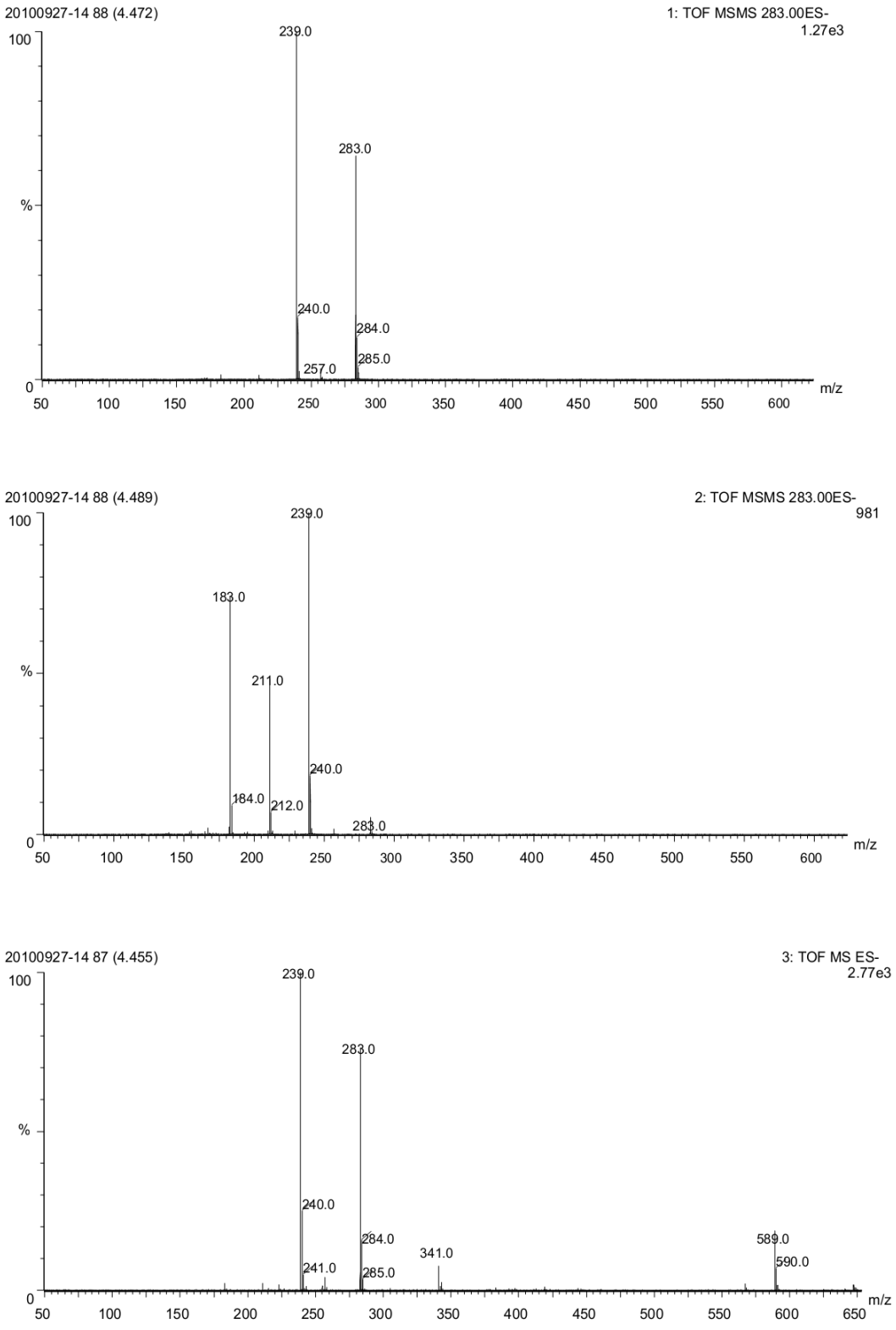

Fig. 1. Mass spectrum for elution1 of the rust spots

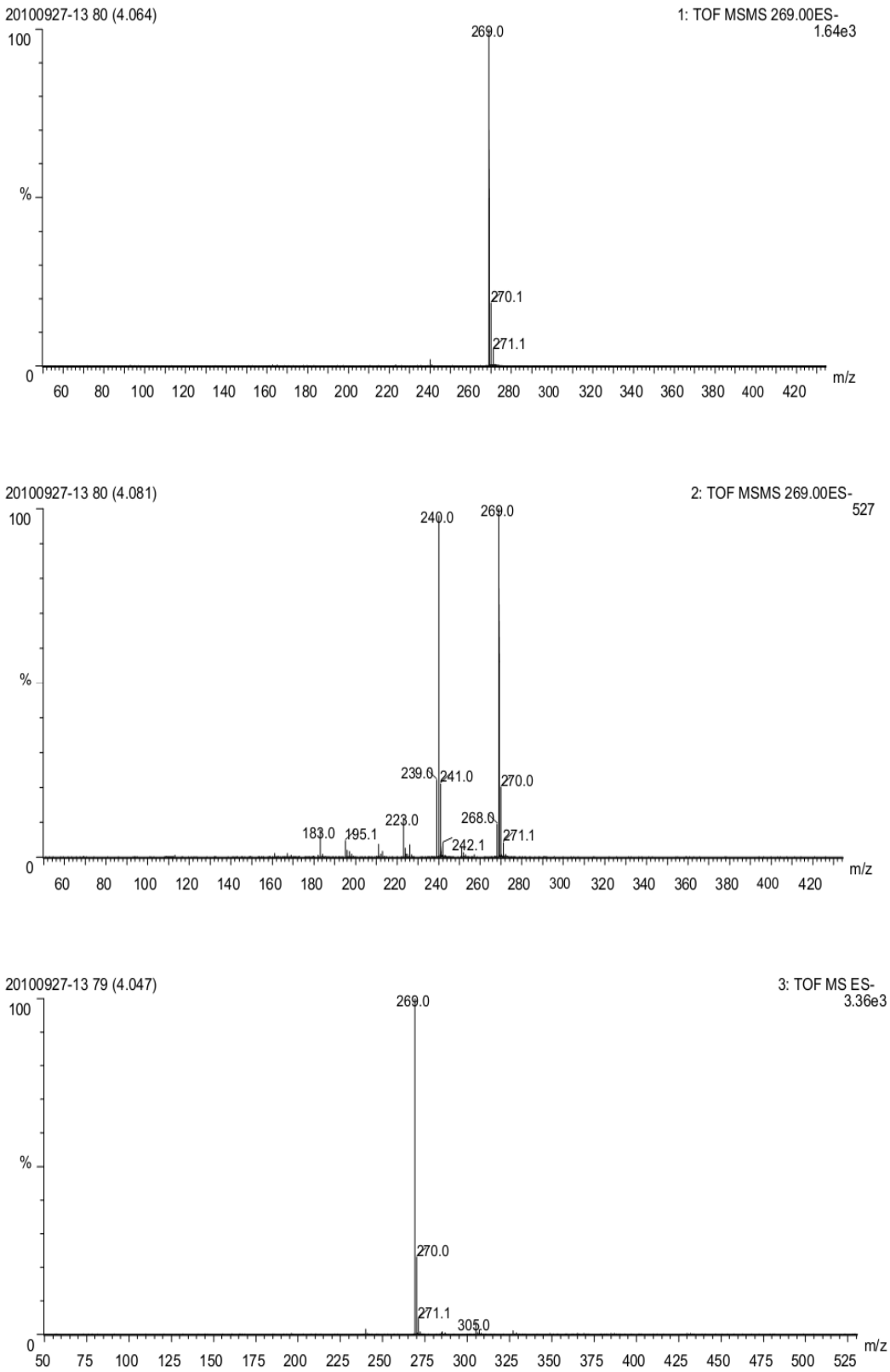

Fig. 2. Mass spectrum for elution 2 of the rust spots

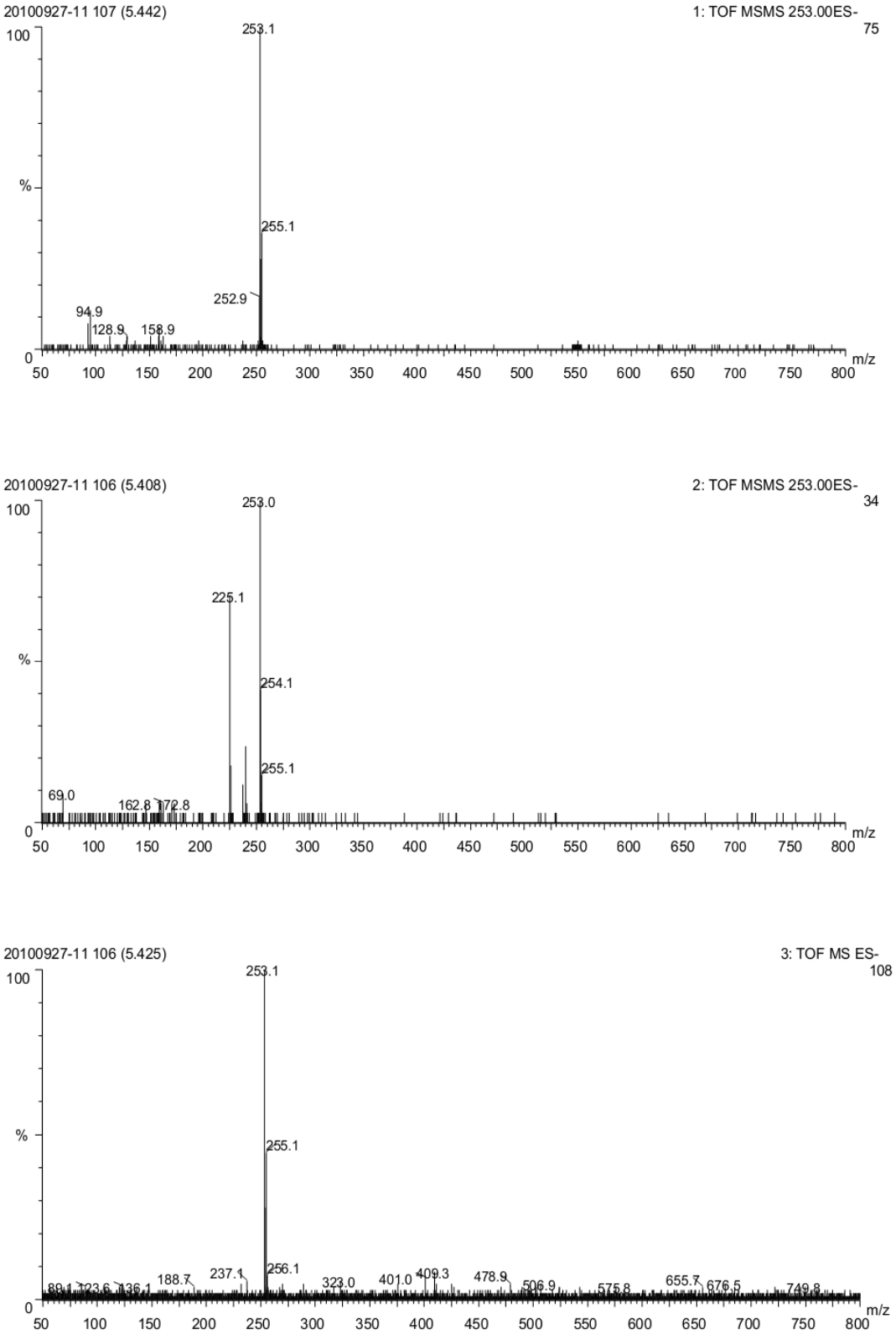

Fig. 3. Mass spectrum for elution 3 of the rust spots

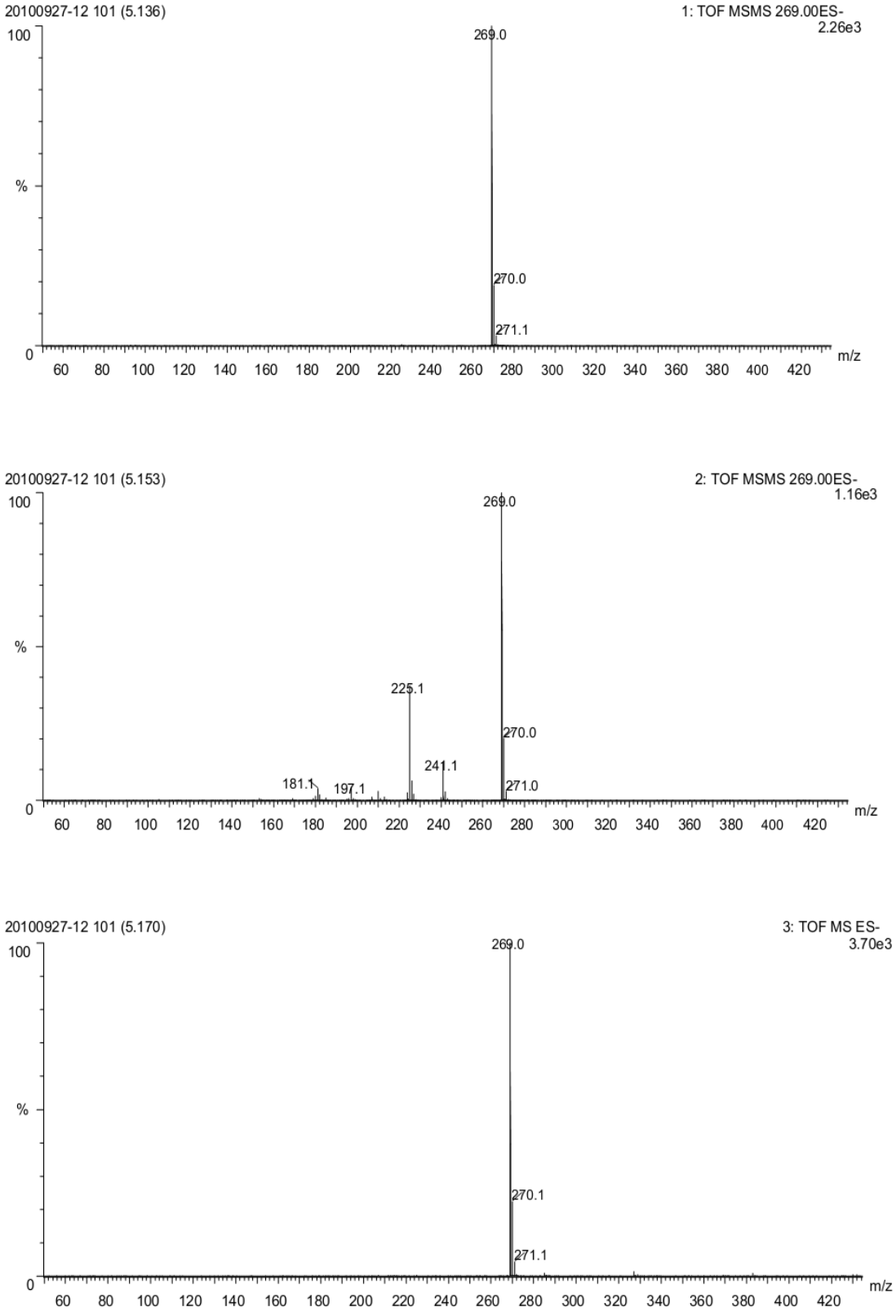

Fig. 4. Mass spectrum for elution 4 of the rust spots

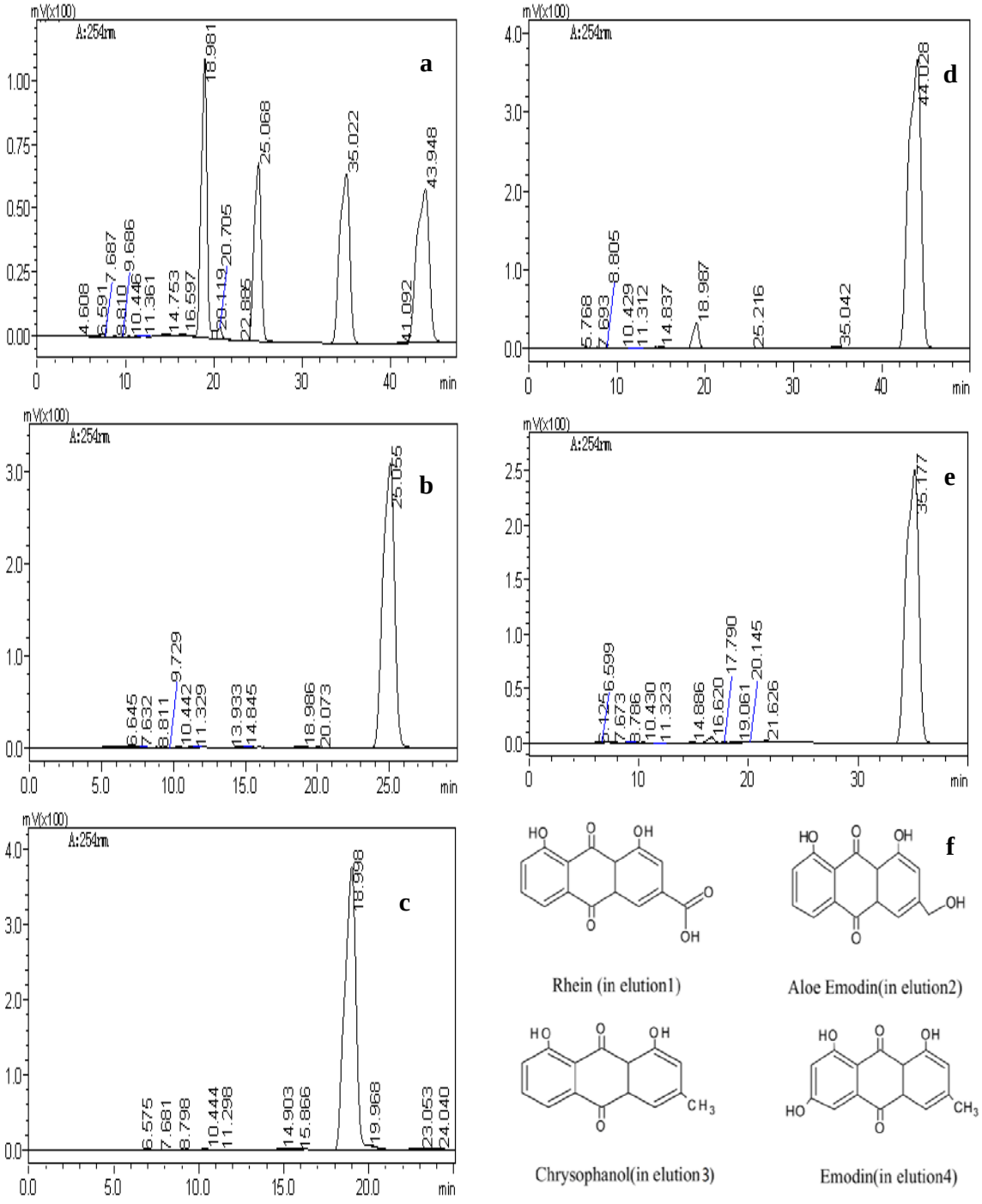

Fig. 5. Liquid chromatogram for rust spots elutions; **a** Liquid chromatogram for standard sample; **b** Liquid chromatogram for rust spots elution 1; **c** Liquid chromatogram for rust spots elution 2; **d** Liquid chromatogram for rust spots elution 3; **e** Liquid chromatogram for rust spots elution 4; **f** Molecular structures of rhein, aloe-emodin, chrysophanol and emodin

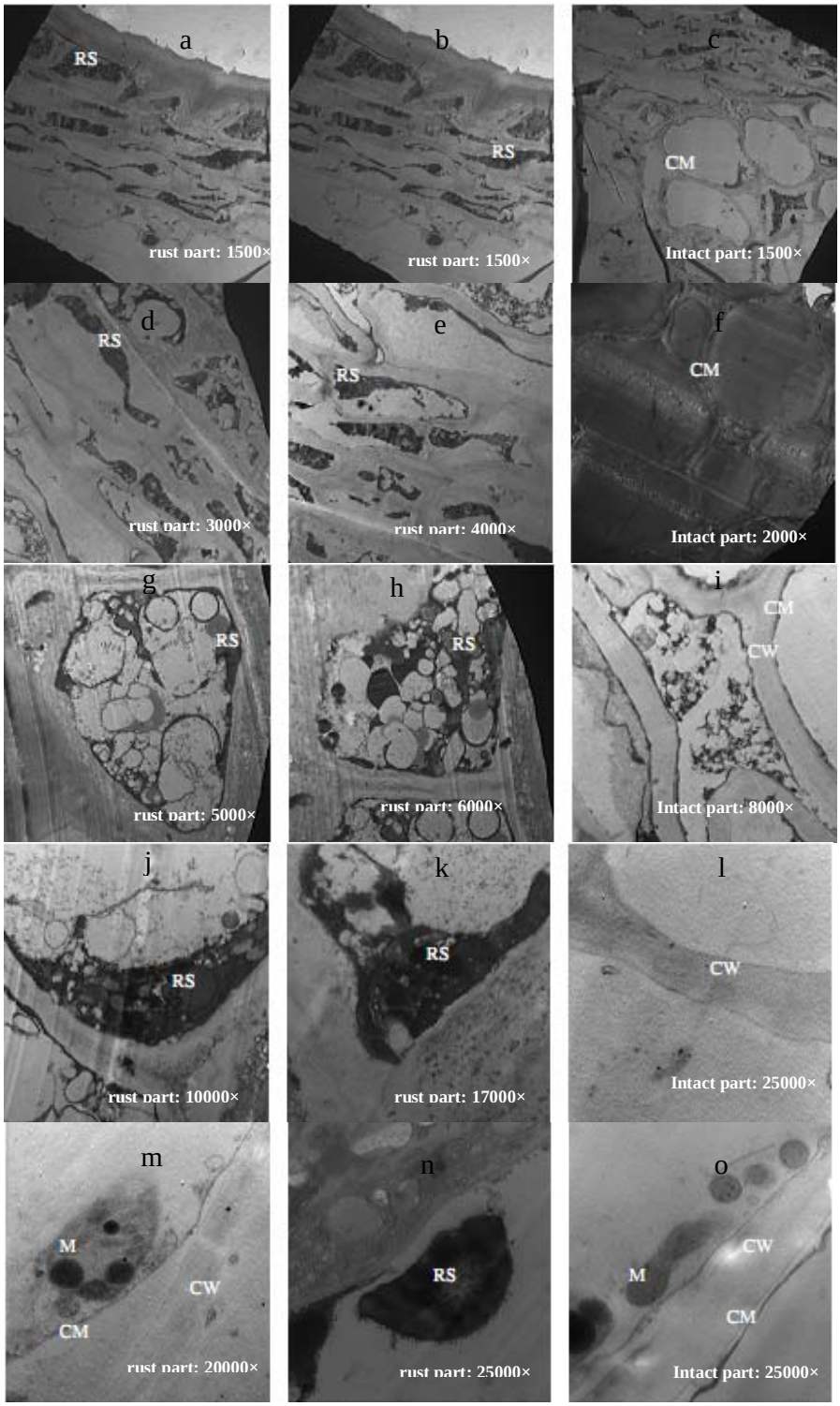

Fig.6 The cell ultrastructure of the rust and intact parts

Note: RS-rust; CW-cell wall; CM-cell membrane; M-mitochondria